Fast and noise-resistant implementation of quantum phase gates and creation of quantum entangled states

Ye-Hong Chen,[1] Yan Xia,[1,*] Qing-Qin Chen,[2] and Jie Song[3]

[1]*Department of Physics, Fuzhou University, Fuzhou 350002, China*
[2]*Zhicheng College, Fuzhou University, Fuzhou 350002, China*
[3]*Department of Physics, Harbin Institute of Technology, Harbin 150001, China*
(Received 30 October 2014; published 20 January 2015)

The "Lewis-Riesenfeld phases" which play a crucial role in constructing shortcuts to adiabaticity may be a resource for the implementation of quantum phase gates. By combining "Lewis-Riesenfeld invariants" with "quantum Zeno dynamics," we propose an effective scheme of rapidly implementing π phase gates via constructing shortcuts to adiabatic passage in a two-distant-atom-cavity system. The influence of various decoherence processes such as spontaneous emission and photon loss on the fidelity is discussed. It is noted that this scheme is insensitive to both error sources. Additionally, a creation of N-atom cluster states is put forward as a typical example of the applications of the fast and noise-resistant phase gates. The study results show that the shortcuts idea is not only applicable in other logic gates with different systems, but also propagable for many quantum information tasks.

I. INTRODUCTION

The recent development of quantum information processing (QIP) has shed new light on complexity and communication theory. The existing quantum algorithms for specific problems shows that quantum computers can in principle solve computational problems much more efficiently than classical computers [1–7]. So far, a lot of studies on the theoretical and practical aspects of quantum computation have been triggered in recent years [8,9]. It has been shown that the key ingredients of achieving quantum computation are quantum logic gates. Using one-qubit and two-qubit logic gates, a universal quantum computation network will be constructed. That is, any unitary transformation, including multiqubit gates, can be decomposed into a series of single qubit operations along with two-qubit logic gates [10,11] in principle. Therefore, this concept has intensively motivated the researches in the realization of the one-qubit unitary gates and the two-qubit logic gates in many physical systems [8–17]. Among them, the cavity quantum electrodynamics (QED) systems, which open up new prospects in the implementation of large-scale quantum computation and generation of nonclassical states with the atoms trapped in optical cavities, have recently become very promising and highly inventive for QIP [18–21]. And there have been tremendous advances in experiments realizing cavity QED systems during the past few years, for example, single cesium atoms have been cooled and trapped in a small optical cavity in the strong-coupling regime [22–24]; quantum computations have been realized in cavity QED systems [12,25]. On the other hand, based on cavity QED systems, lots of theoretical schemes [26–32] have been proposed to implement two-qubit logic gates with trapped atoms. For instance, Zheng implemented a π phase gate through the adiabatic evolution in 2005 [30]. The procedure of acquiring the quantum phase gate is simplified because

the scheme's system was not required to undergo a desired cyclic evolution. And the fidelity for the scheme was said to be improved due to the avoidance of the errors. The paper aroused a great deal of interest in using adiabatic evolution to implement phase gates [33–36].

However, the adiabatic condition limits the speed of the evolution of the system. The previous methods based on the adiabatic passage technique usually require a relatively long interaction time. In general, the interaction time for a method is the shorter the better, otherwise, the method may be useless because the dissipation caused by decoherence, noise, and losses on the target state increases with the increasing of the interaction time. Therefore, finding shortcuts to adiabaticity is of great significance for QIP and has drawn much more attention than ever before. In recent years, various reliable, fast, and robust schemes have been proposed in finding shortcuts to a slow adiabatic passage in both theory [37–44] and experiment [45–50]. For example, Chen and Muga constructed shortcuts by invariant-based inverse engineering to perform fast population transfer in three-level systems in 2012 [42]. Lu *et al.* constructed shortcuts by using the approach of "transitionless quantum driving" to the population transfer and the creation of maximal entanglement in the cavity QED system [51]. In 2014, motivated by the quantum Zeno dynamics [52,53], Chen *et al.* constructed shortcuts to perform the fast populations transfer of ground states in multiparticle systems with the invariant-based inverse engineering [54]. Soon after that, they generalized their method into distant cavities to realize fast and noise-resistant QIP, including quantum population transfer, entangled states preparation and transition [55].

Refs. [37,38,42–44,54] prove that constructing shortcuts always has to deal with the quantum phases transition, for example, the Berry phases [44], the Lewis-Riesenfeld (LR) [56] phases, and so on. In view of that we wonder if it is possible to use shortcuts to adiabatic passage (STAPs) for the implementation of logic gates. Therefore, in this paper, we effectively construct STAPs in a two-distant-atom system to implement π phase gates through designing resonant laser pulses by the invariant-based inverse engineering. The logic gates can be

*xia-208@163.com

achieved in a much shorter interaction time via STAPs than that based on adiabatic passage and the interaction time also not needs to be controlled accurately. Similar to the adiabatic passage, the present scheme is insensitive to variations of the parameters. Moreover, because of the short interaction time, the present scheme is insensitive to the decoherence caused by spontaneous emission and photon loss even though we increase the populations of some excited states during the gate operation. And we also give an example of applications of this kind of phase gates: using the fast and noise-resistant gates to create N-atom cluster states in spatially separated cavities.

This paper is structured as follows. In Sec. II, we briefly describe the LR phases. In Sec. III, we construct STAPs in a two-distant-atom system by the invariant-based inverse engineering, and show how to use the shortcut to implement π phase gates. Then, in Sec. IV we use the kind of phase gates to create N-atom cluster states in N distant cavities connected by $N-1$ fibers. We give the numerical simulation and experimental discussion about the validity of the scheme in Sec. V, and Sec. VI is the conclusion.

II. LEWIS-RIESENFELD PHASES

A brief description about the LR theory [56] is given in this section. We consider a time-dependent quantum system whose Hamiltonian is $H(t)$. Associated with the Hamiltonian, there are time-dependent Hermitian invariants of motion $I(t)$ that satisfy

$$i\hbar\partial_t I(t) - [H(t), I(t)] = 0, \tag{1}$$

where $\partial_t \equiv \frac{\partial}{\partial t}$. For any solution $|\Psi(t)\rangle$ of the time-dependent Schrödinger equation $i\hbar\partial_t|\Psi(t)\rangle = H(t)|\Psi(t)\rangle$, $I|\Psi(t)\rangle$ is also a solution [57], and $|\Psi(t)\rangle$ can be expressed as a linear combination of invariant modes,

$$|\Psi(t)\rangle = \sum_n C_n e^{i\alpha_n}|\phi_n(t)\rangle, \tag{2}$$

where C_n are constants, $|\phi_n(t)\rangle$ is the nth eigenvector of $I(t)$, and the corresponding real eigenvalue is λ_n. The LR phases α_n fulfill

$$\hbar\frac{d\alpha_n}{dt} = \langle\phi_n(t)|i\hbar\partial_t - H(t)|\phi_n(t)\rangle. \tag{3}$$
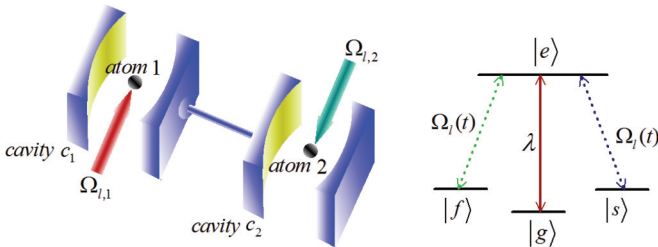

FIG. 1. (Color online) The cavity-fiber-atom combined system and the atomic level configuration for the implementation of phase gates.

III. SHORTCUT TO ADIABATICITY FOR TWO-QUBIT π PHASE GATES

We consider that two four-level atoms (1 and 2) are respectively trapped in two cavities (c_1 and c_2) connected by a fiber as shown in Fig. 1. Each atom has three ground states $|g\rangle$, $|f\rangle$, and $|s\rangle$, and an excited state $|e\rangle$. The whole system evolves in the one-excited subspace spanned by

$$
\begin{aligned}
|\psi_1\rangle &= |f\rangle_1|g\rangle_2|0\rangle_{c_1}|0\rangle_{c_2}|0\rangle_f, \\
|\psi_2\rangle &= |e\rangle_1|g\rangle_2|0\rangle_{c_1}|0\rangle_{c_2}|0\rangle_f, \\
|\psi_3\rangle &= |g\rangle_1|g\rangle_2|1\rangle_{c_1}|0\rangle_{c_2}|0\rangle_f, \\
|\psi_4\rangle &= |g\rangle_1|g\rangle_2|0\rangle_{c_1}|0\rangle_{c_2}|1\rangle_f, \\
|\psi_5\rangle &= |g\rangle_1|g\rangle_2|0\rangle_{c_1}|1\rangle_{c_2}|0\rangle_f, \\
|\psi_6\rangle &= |g\rangle_1|e\rangle_2|0\rangle_{c_1}|0\rangle_{c_2}|0\rangle_f, \\
|\psi_7\rangle &= |g\rangle_1|f\rangle_2|0\rangle_{c_1}|0\rangle_{c_2}|0\rangle_f, \\
|\psi_8\rangle &= |s\rangle_1|g\rangle_2|0\rangle_{c_1}|0\rangle_{c_2}|0\rangle_f, \\
|\psi_9\rangle &= |g\rangle_1|s\rangle_2|0\rangle_{c_1}|0\rangle_{c_2}|0\rangle_f.
\end{aligned}
\tag{4}
$$

We assume that the atomic transition $|f\rangle \leftrightarrow |e\rangle$ is resonantly driven through a time-dependent laser pulse with Rabi frequency $\Omega_l(t)$, transition $|s\rangle \leftrightarrow |e\rangle$ is resonantly driven through a time-dependent laser pulse with Rabi frequency $\Omega_r(t)$, the transition $|g\rangle \leftrightarrow |e\rangle$ is resonantly coupled to the cavity mode with coupling constant λ. In the short fiber limit $L\tau/(2\pi c) \ll 1$ [58,59], where L denotes the fiber length, c denotes the speed of light, and τ denotes the decay of the cavity field into a continuum of fiber mode, the cavities c_1 and c_2 are coupled to one fiber mode with strength v. We turn off the classical laser fields $\Omega_{r,k}$ ($k = 1,2$) at first. The Hamiltonian of the system in interaction picture for this case can be written as ($\hbar = 1$)

$$
\begin{aligned}
H_i(t) &= H_{al} + H_{ac} + H_{cf}, \\
H_{al}(t) &= \sum_{k=1,2} \Omega_{l,k}(t)|e\rangle_k\langle f| + \text{H.c.}, \\
H_{ac}(t) &= \sum_{k=1,2} \lambda_k a_k|e\rangle_k\langle g| + \text{H.c.}, \\
H_{cf}(t) &= v b^\dagger(a_1 + a_2) + \text{H.c.},
\end{aligned}
\tag{5}
$$

where the subscript k represents the kth atom and a_k is the annihilation operator for the kth cavity mode, and $b^\dagger$ represents the creation operator of the fiber mode. Considering quantum Zeno dynamics, we set $\Omega_{l,k}(t) \ll \lambda$ (the Zeno condition) and rewrite the Hamiltonian in Eq. (5) with the eigenvectors of Hamiltonian H_{im} ($H_{im} = H_{ac} + H_{cf}$) as ($g_1 = g_2 = g$ and $\chi = \sqrt{2v^2 + \lambda^2}$)

$$
\begin{aligned}
H_I &= \sum_{m=0}^4 \xi_m|\theta_m\rangle\langle\theta_m| + \left[\frac{v}{\chi}|\theta_0\rangle(\Omega_{l,1}\langle\psi_1| + \Omega_{l,2}\langle\psi_7|)\right. \\
&\quad + \frac{1}{2}(|\theta_1\rangle + |\theta_2\rangle)(-\Omega_{l,1}\langle\psi_1| + \Omega_{l,2}\langle\psi_7|) \\
&\quad \left. + \frac{\lambda}{2\chi}(|\theta_3\rangle + |\theta_4\rangle)(\Omega_{l,1}\langle\psi_1| + \Omega_{l,2}\langle\psi_7|) + \text{H.c.}\right],
\end{aligned}
\tag{6}
$$

where

$$|\theta_0\rangle = \frac{v}{\chi}\left(|\psi_2\rangle - \frac{\lambda}{v}|\psi_4\rangle + |\psi_6\rangle\right),$$

$$|\theta_1\rangle = \frac{1}{2}(-|\psi_2\rangle - |\psi_3\rangle + |\psi_5\rangle + |\psi_6\rangle),$$

$$|\theta_2\rangle = \frac{1}{2}(-|\psi_2\rangle + |\psi_3\rangle - |\psi_5\rangle + |\psi_6\rangle), \tag{7}$$

$$|\theta_3\rangle = \frac{\lambda}{2\chi}\left(|\psi_2\rangle + \frac{\chi}{\lambda}|\psi_3\rangle + \frac{2v}{\lambda}|\psi_4\rangle + \frac{\chi}{\lambda}|\psi_5\rangle + |\psi_6\rangle\right),$$

$$|\theta_4\rangle = \frac{\lambda}{2\chi}\left(|\psi_2\rangle - \frac{\chi}{\lambda}|\psi_3\rangle + \frac{2v}{\lambda}|\psi_4\rangle - \frac{\chi}{\lambda}|\psi_5\rangle + |\psi_6\rangle\right)$$

are the eigenvectors of H_{im} corresponding eigenvalues $\xi_0 = 0, \xi_1 = \lambda, \xi_2 = -\lambda, \xi_3 = \chi$, and $\xi_4 = -\chi$, respectively. Perform the unitary transformation $U = e^{-i(\sum_{m=0}^{4}\xi_m|\theta_m\rangle\langle\theta_m|)t}$, and we obtain

$$\begin{aligned}H_{\text{app}} = &\frac{1}{2}(e^{i\lambda t}|\theta_1\rangle + e^{-i\lambda t}|\theta_2\rangle)(-\Omega_{l,1}\langle\psi_1| + \Omega_{l,2}\langle\psi_7|)\\ &+ \frac{\lambda}{2\chi}(e^{i\chi t}|\theta_3\rangle + e^{-i\chi t}|\theta_4\rangle)(\Omega_{l,1}\langle\psi_1| + \Omega_{l,2}\langle\psi_7|)\\ &+ \frac{v}{\chi}|\theta_0\rangle(\Omega_{l,1}\langle\psi_1| + \Omega_{l,2}\langle\psi_7|) + \text{H.c.}\end{aligned} \tag{8}$$

Neglecting the terms with high oscillating frequencies λ and χ then the final effective Hamiltonian is obtained,

$$\begin{aligned}H_{\text{eff}} &= \frac{v}{\chi}|\theta_0\rangle(\Omega_{l,1}\langle\psi_1| + \Omega_{l,2}\langle\psi_7|) + \text{H.c.}\\ &= \frac{v}{\chi}\begin{pmatrix} 0 & \Omega_{l,1}(t) & 0 \\ \Omega_{l,1}(t) & 0 & \Omega_{l,2}(t) \\ 0 & \Omega_{l,2}(t) & 0 \end{pmatrix}.\end{aligned} \tag{9}$$

It is obvious that H_{eff} possesses SU(2) dynamical symmetry [60], and the invariant $I(t)$ is given by [41,54]

$$\begin{aligned}I(t) &= \frac{v}{\chi}\omega_0[|\theta_0\rangle(\cos\gamma\sin\beta\langle\psi_1| + \cos\gamma\cos\beta\langle\psi_7|)\\ &\quad - i\sin\gamma|\psi_7\rangle\langle\psi_1|] + \text{H.c.}\\ &= \frac{v}{\chi}\omega_0\begin{pmatrix} 0 & \cos\gamma\sin\beta & -i\sin\gamma \\ \cos\gamma\sin\beta & 0 & \cos\gamma\cos\beta \\ i\sin\gamma & \cos\gamma\cos\beta & 0 \end{pmatrix},\end{aligned} \tag{10}$$

where ω_0 is an arbitrary constant with units of frequency to keep $I(t)$ with dimensions of energy. By solving the differential equation in Eq. (1), the time-dependent Rabi frequencies $\Omega_{l,1}(t)$ and $\Omega_{l,2}(t)$ are given,

$$\begin{aligned}\Omega_{l,1}(t) &= \frac{\chi}{v}(\dot{\beta}\cot\gamma\sin\beta + \dot{\gamma}\cos\beta),\\ \Omega_{l,2}(t) &= \frac{\chi}{v}(\dot{\beta}\cot\gamma\cos\beta - \dot{\gamma}\sin\beta).\end{aligned} \tag{11}$$

and the eigenstates of $I(t)$, with eigenvalues $\lambda_0 = 0$ and $\lambda_\pm = \pm 1$, are

$$|\phi_0(t)\rangle = \begin{pmatrix} \cos\gamma\cos\beta \\ -i\sin\gamma \\ -\cos\gamma\sin\beta \end{pmatrix},$$

$$|\phi_\pm(t)\rangle = \frac{1}{\sqrt{2}}\begin{pmatrix} \sin\gamma\cos\beta \pm i\sin\beta \\ i\cos\gamma \\ -\sin\gamma\sin\beta \pm i\cos\beta \end{pmatrix}. \tag{12}$$

In order to achieve fast adiabaticlike process (a process which is not really adiabatic but leading to the same final populations), we impose relations $[I(0), H_{\text{eff}}(0)] = 0$ and $[I(t_f), H_{\text{eff}}(t_f)] = 0$, where t_f is the total interaction time. Thus, we obtain the boundary conditions $\dot{\gamma}(0) = \dot{\gamma}(t_f) = 0$, and the LR phases,

$$\alpha_0 = 0,$$

$$\alpha_\pm = \mp\int_0^{t_f}\left[\dot{\beta}\sin\gamma + \frac{v}{\chi}(\Omega_{l,1}\sin\beta + \Omega_{l,2}\cos\beta)\cos\gamma\right]dt. \tag{13}$$

Moreover, the constants C_n ($n = 0,\pm$) also can be given through the relation $C_n = \langle\phi_n(0)|\psi_1\rangle$. Generating a π phase change of the quantum states involved in such a system, the final state should become $-|\psi_1\rangle$. Therefore, we choose the feasible parameters $\gamma(t) = \epsilon$ and $\beta(t) = \pi t/t_f$, where ϵ is a small value. We obtain

$$\begin{aligned}\Omega_{l,1}(t) &= \Omega_0\sin\beta,\\ \Omega_{l,2}(t) &= \Omega_0\cos\beta,\end{aligned} \tag{14}$$

and the final state

$$|\Psi(t_f)\rangle = \begin{pmatrix} -\cos^2\epsilon - \cos\alpha\sin^2\epsilon \\ -i\sin\epsilon\cos\epsilon + i\cos\alpha\sin\epsilon\cos\epsilon \\ \sin\epsilon\sin\alpha \end{pmatrix}, \tag{15}$$

where $\alpha = \pi/(2\sin\epsilon)$ and $\Omega_0 = \chi\pi\cot\epsilon/(vt_f)$. When we choose $(\sin\epsilon)^{-1} = 4\zeta$ ($\zeta = 1,2,3,\ldots$), $\cos\alpha = 1$ and the final state becomes $|\Psi(t_f)\rangle = [-1,0,0]' = -|\psi_1\rangle$.

If the initial state of the system is $|f\rangle_1|s\rangle_2|0\rangle_c$, the whole system evolves in a subspace spanned by

$$\begin{aligned}|\varphi_1\rangle &= |f\rangle_1|s\rangle_2|0\rangle_{c_1}|0\rangle_{c_2}|0\rangle_f,\\ |\varphi_2\rangle &= |e\rangle_1|s\rangle_2|0\rangle_{c_1}|0\rangle_{c_2}|0\rangle_f,\\ |\varphi_3\rangle &= |g\rangle_1|s\rangle_2|1\rangle_{c_1}|0\rangle_{c_2}|0\rangle_f,\\ |\varphi_4\rangle &= |g\rangle_1|s\rangle_2|0\rangle_{c_1}|0\rangle_{c_2}|1\rangle_f,\\ |\varphi_5\rangle &= |g\rangle_1|s\rangle_2|0\rangle_{c_1}|1\rangle_{c_2}|0\rangle_f,\end{aligned} \tag{16}$$

and the interaction picture Hamiltonian is

$$H_{i,s} = \Omega_{l,1}|\varphi_2\rangle\langle\varphi_1| + \lambda|\varphi_2\rangle\langle\varphi_3| + v|\varphi_4\rangle(\langle\varphi_3| + \langle\varphi_5|) + \text{H.c.} \tag{17}$$

With the parameters above, the adiabatic condition $\langle\tilde{\theta}_0|\partial_t\tilde{\theta}_\pm\rangle \ll \tilde{\xi}_\pm$ for this subspace is fulfilled, where $|\tilde{\theta}_0\rangle$ is the eigenstate corresponding eigenvalue $\tilde{\xi}_0 = 0$, and $|\tilde{\theta}_\pm\rangle$ are the eigenstates corresponding nonzero eigenvalues $\tilde{\xi}_\pm$. And if the initial state of system is $|\tilde{\theta}_0(0)\rangle$, it evolves along the dark

state

$$|\tilde{\theta}_0(t)\rangle = \frac{1}{\sqrt{2\Omega_{l,1}^2 + \lambda^2}}(\lambda|\varphi_1\rangle - \Omega_{l,1}(t)|\varphi_3\rangle + \Omega_{l,1}(t)|\varphi_5\rangle).$$

(18)

When $t = t_f$, $\Omega_{l,1}(t_f) = 0$ and the final state becomes $|\tilde{\theta}_0(t_f)\rangle = |\varphi_1\rangle$.

It is obvious that the total Hamiltonian H_i has no effect on the evolution of initial states $|g\rangle_1|s\rangle_2|0\rangle_{c_1}|0\rangle_{c_2}|0\rangle_f$ and $|g\rangle_1|g\rangle_2|0\rangle_{c_1}|0\rangle_{c_2}|0\rangle_f$,

$$H_i|g\rangle_1|s\rangle_2|0\rangle_{c_1}|0\rangle_{c_2}|0\rangle_f = 0,$$
$$H_i|g\rangle_1|g\rangle_2|0\rangle_{c_1}|0\rangle_{c_2}|0\rangle_f = 0.$$

(19)

Therefore, we have

$$|g,s\rangle_{1,2}|0,0,0\rangle_{c_1,c_2,f} \rightarrow |g,s\rangle_{1,2}|0,0,0\rangle_{c_1,c_2,f},$$
$$|g,g\rangle_{1,2}|0,0,0\rangle_{c_1,c_2,f} \rightarrow |g,g\rangle_{1,2}|0,0,0\rangle_{c_1,c_2,f},$$
$$|f,s\rangle_{1,2}|0,0,0\rangle_{c_1,c_2,f} \rightarrow |f,s\rangle_{1,2}|0,0,0\rangle_{c_1,c_2,f},$$
$$|f,g\rangle_{1,2}|0,0,0\rangle_{c_1,c_2,f} \rightarrow -|f,g\rangle_{1,2}|0,0,0\rangle_{c_1,c_2,f},$$

(20)

which is a π phase gate.

IV. PREPARATION OF CLUSTER STATES

To demonstrate the possible application of the phase gate proposed in Sec. III, we will show that we can use the gate to create cluster states. As shown in Fig. 2, N atoms (1, 2, 3, ..., N) are trapped in N cavities ($c_1, c_2, ..., c_N$) connected by $N - 1$ fibers and optical switches [61], respectively. All the optical switches ($O_1, O_2, ..., O_{N-1}$) are turned off in the beginning to void interaction with each atom. Then, we turn on the optical switch O_1 to let the the optical fiber mediate the cavities c_1 and c_2. And we prepare the atoms 1 and 2 in the state $|\varpi_1\rangle = \frac{1}{2}(|f\rangle_1 + |g\rangle_1)(|s\rangle_2 + |g\rangle_2)$. Using the π phase gate achieved above in Sec. III, we easily obtain a two-atom state as follows:

$$|\varpi_1'\rangle = \frac{1}{2}(|f,s\rangle_{1,2} - |f,g\rangle_{1,2} + |g,s\rangle_{1,2} + |g,g\rangle_{1,2})$$
$$= \frac{1}{2}(|f\rangle_1\sigma_2^z + |g\rangle_1)(|s\rangle_2 + |g\rangle_2),$$

(21)

where $\sigma_2^z = |s\rangle_2\langle s| - |g\rangle_2\langle g|$. Then we turn off the optical switch O_1 and turn on O_2. Meanwhile, atom 3 is prepared in state $\frac{1}{\sqrt{2}}(|f\rangle_3 + |g\rangle_3)$. In this case, the whole atomic system is

$$|\varpi_2\rangle = \frac{1}{2}(|f\rangle_1\sigma_2^z + |g\rangle_1)(|s\rangle_2 + |g\rangle_2) \otimes \frac{1}{\sqrt{2}}(|f\rangle_3 + |g\rangle_3).$$

(22)

Afterward, we turn off laser pulse $\Omega_{l,k}$ (here $k = 2,3$) and turn on the laser pulses $\Omega_{r,k}$. It is obvious that the behavior of Ω_r
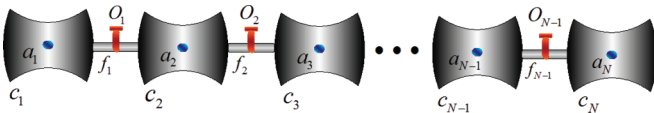

FIG. 2. (Color online) The setup diagram for the creation of cluster states.

are the same as that of Ω_l. The Hamiltonian for the whole system can be expressed as

$$H_{i,2}(t) = vb_2^\dagger(a_2 + a_3) + \sum_{k=2,3}\Omega_{r,k}(t)|e\rangle_k\langle s|$$
$$+ \lambda_k a_k|e\rangle_k\langle g| + \text{H.c.},$$

(23)

which is similar to the Hamiltonian in Eq. (5). Therefore, by using the same method in Sec. III (setting $\Omega_{r,2} = \Omega_{l,1}$ and $\Omega_{r,3} = \Omega_{l,2}$), we achieve another π phase gate:

$$|g,f\rangle_{2,3}|0,0,0\rangle_{c_2,c_3,f_2} \rightarrow |g,f\rangle_{2,3}|0,0,0\rangle_{c_2,c_3,f_2},$$
$$|g,g\rangle_{2,3}|0,0,0\rangle_{c_2,c_3,f_2} \rightarrow |g,g\rangle_{2,3}|0,0,0\rangle_{c_2,c_3,f_2},$$
$$|s,f\rangle_{2,3}|0,0,0\rangle_{c_2,c_3,f_2} \rightarrow |s,f\rangle_{2,3}|0,0,0\rangle_{c_2,c_3,f_2},$$
$$|s,g\rangle_{2,3}|0,0,0\rangle_{c_2,c_3,f_2} \rightarrow -|s,g\rangle_{2,3}|0,0,0\rangle_{c_2,c_3,f_2}.$$

(24)

Using this phase gate, the state $|\varpi_2\rangle$ becomes a three-atom cluster state:

$$|\varpi_2'\rangle = \frac{1}{\sqrt{2}}(|f\rangle_1\sigma_2^z + |g\rangle_1)\frac{1}{2}(|s,f\rangle_{2,3}$$
$$- |s,g\rangle_{2,3} + |g,f\rangle_{2,3} + |g,g\rangle_{2,3})$$
$$= \frac{1}{2\sqrt{2}}(|f\rangle_1\sigma_2^z + |g\rangle_1)(|s\rangle_2\sigma_3^z + |g\rangle_2)(|f\rangle_3 + |g\rangle_3),$$

(25)

where $\sigma_3^z = |f\rangle_3\langle f| - |g\rangle_3\langle g|$. The rest may be deduced by analogy. Once an $(M - 1)$-atom ($2 \leqslant M \leqslant N$) cluster state has been generated, an M-atom cluster state can be easily created by the following four steps:

(1) Turn on the optical switch O_{M-1} (other optical switches are all kept off).

(2) (a) If M is an odd number, the atom M should be prepared in state $\frac{1}{\sqrt{2}}(|f\rangle_M + |g\rangle_M)$, the laser pluses $\Omega_{r,M}$ and $\Omega_{r,M-1}$ should be turned on. (b) If M is an even number, the atom M should be prepared in state $\frac{1}{\sqrt{2}}(|s\rangle_M + |g\rangle_M)$, the laser pluses $\Omega_{l,M}$ and $\Omega_{l,M-1}$ should be turned on.

(3) Use the same method as in Sec. III to implement the π phase gate operation.

(4) The M-atom cluster state can be generated through the above three steps.

V. NUMERICAL SIMULATION AND DISCUSSION

The validity of the above theoretical analysis will be numerically proved in the following. From Eq. (14), we know that the amplitude of the laser pulse is

$$\Omega_0 = \frac{\chi\pi\cot\epsilon}{vt_f} = \frac{\pi\cot\epsilon}{t_f}\sqrt{2 + (\lambda/v)^2}.$$

(26)

That is, the amplitude of the laser pulse depends on three parameters: ϵ, t_f, and v. And there is an inverse relationship between Ω_0 and t_f (v) when ϵ is a constant value. Figure 3(a) shows the fidelity of the target state $-|\psi_1\rangle$ versus parameters λt_f and v/λ in the case of $\epsilon = \arcsin 0.25$. From the figure, we find that, when $t_f = 20/\lambda$ and $v = 0.7\lambda$, the fidelity is also higher than 90%, while with these two parameters, the laser amplitude is $\Omega_0 = 1.22$ which does not meet the Zeno condition $\Omega_{l,k} \ll \lambda$. The reason for this result has been discussed in Refs. [54,55] in detail: the population transfer
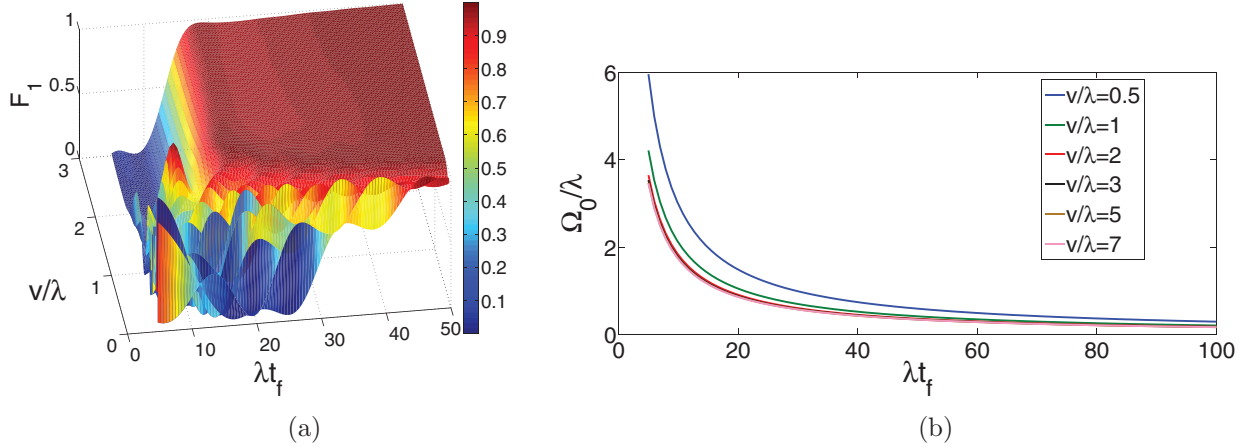
FIG. 3. (Color online) (a) The fidelity F_1 of the target state $-|\psi_1\rangle$ vs the λt_f and the hopping rate v/λ. (b) The laser amplitude Ω_0/λ vs the λt_f with different hopping rates v/λ.

form the initial state $|\psi_1\rangle$ to the target state $|\psi_7\rangle$ can be fast and perfectly achieved even when the Zeno condition has not been fulfilled and vice versa. However, in this paper, we focus on how to use the LR phases to implement a π phase gate. From the theoretical analysis above, we know that when the Zeno condition is destroyed, the phase change of the whole system is unpredictable and unanalyzable. Therefore, through the relationship in Eq. (26), we plot in Fig. 3(b) the case of $\epsilon = \arcsin 0.25$ to accurately choose v and t_f to make sure the Zeno condition is fulfilled. The result shows that when t_f or v is large enough, Ω_0 only changes a little with the changing of t_f or v. To complete the gate operation in a short interaction time, it seems that $t_f = 50/\lambda$ and $v = 2\lambda$ is a good choice for the scheme. The above analysis is based on ϵ as a constant value, while we know that there are also some different choices for the parameter ϵ as shown in Fig. 4. Figure 4 is plotted with $\{t_f = 50/\lambda, \ v = 2\lambda\}$, and we find that the ideal value of ϵ for the highest fidelity is slightly different from the condition $\epsilon = \arcsin 1/\zeta$; the reason for this difference has been discussed in Ref. [54] in detail: in the present case, the Zeno condition is satisfied but not very ideally because speeding up the system requires relatively large laser intensities. Therefore, under the premise that the interaction time for the gate operation is short, to satisfy the Zeno condition as well as possible, the parameters for Ω_0 are chosen as $\{\epsilon = 0.258, \ v = 2\lambda, \ t_f = 50/\lambda\}$. With these parameters, as shown in Fig. 5(a), the laser pulses are

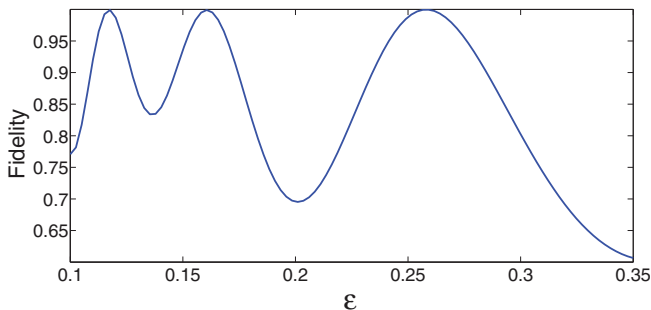determined. And the time evolution of the populations for states $|\psi_1\rangle$, $|\psi_5\rangle$, $|\theta_0\rangle$, $|\theta_1\rangle$ ($|\theta_2\rangle$), and $|\theta_3\rangle$ ($|\theta_4\rangle$) are shown in Fig. 5(b). An obvious phenomenon in the figure which is much different from the adiabatic passage technique is that the intermediate state $|\theta_0\rangle$ is populated during the evolution (in a scheme based on adiabatic passage, the state $|\theta_0\rangle$ is usually neglected). We can understand this from Refs. [37,42,54]; the key point to speed up the population transfer is increasing the intermediate states, especially the states which are neglected during the adiabatic passage. Ideally, the more the intermediate states are populated, the faster the evolution is. However, a high population of an intermediate state usually leads to decoherence of the system. What is more drawn from Fig. 5(b) is that we can confirm that the Zeno condition is fulfilled with this set of parameters: the states $|\theta_1\rangle$, $|\theta_2\rangle$, $|\theta_3\rangle$, and $|\theta_4\rangle$ are all considered as negligible during the evolution. In Fig. 6(a), we show the evolution of the system when the initial state is $|\varphi_1\rangle$. The solid curves which are plotted through the relation $P_j^R = |\langle\varphi_j|\rho_s(t)|\varphi_j\rangle|$ ($j = 1,3,5$) are the time-dependent populations for states $|\varphi_j\rangle$, and the dashed curves which are plotted through the relation $P_j^D = |\langle\varphi_j|\tilde{\theta}_0(t)\rangle|^2$ are also the time-dependent populations for states $|\varphi_j\rangle$, where $\rho_s(t)$ which satisfies $\partial_t\rho_s = i[\rho_s, H_{i,s}]$ is the density operator for the Hamiltonian $H_{i,s}$ in Eq. (17) and $|\tilde{\theta}_0(t)\rangle$ is the dark state in Eq. (18). From this figure, we find there are some differences between the evolutions governed by $H_{i,s}$ and the dark state: it seems that the dark state cannot ideally describe the evolution of the system. Through analyzing Refs. [42,54,55,62] in detail, a favorable inference is drawn: for a resonant Λ-type three-level system as shown in Ref. [62], if the stokes and pump pulses are designed with the forms

$$\Omega_p(t) = \Omega_0 \sin \frac{\beta}{2}, \quad \Omega_s(t) = \Omega_0 \cos \frac{\beta}{2}, \qquad (27)$$

$\zeta = (\sin \epsilon)^{-1}/4$ seems to dominate the oscillation number of the curves which describe the time-dependent populations of the three states. When ζ is too small, for instance, $\zeta = 1,2$, the system cannot meet the adiabatic condition. Numerical simulation shows that, in this Λ-type system, the oscillation number N_o equals ζ. And we draw an inference that at least

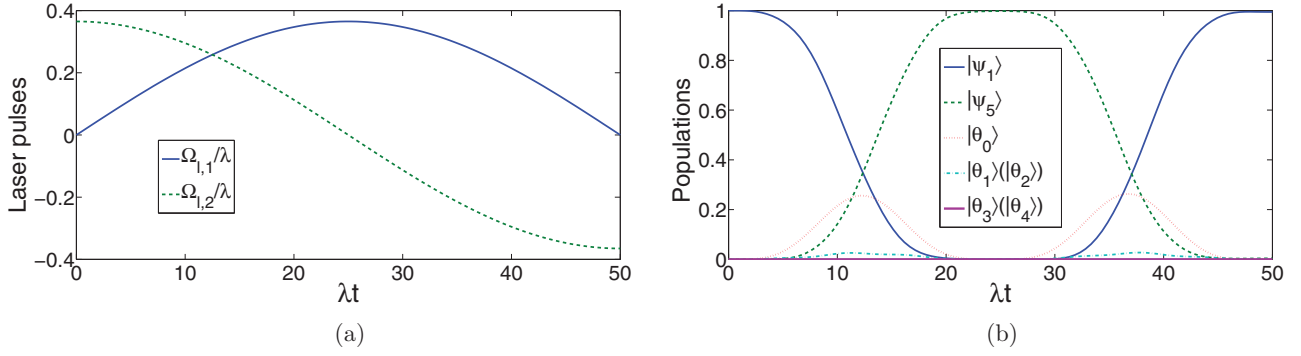FIG. 4. (Color online) The fidelity F_1 vs the parameter ϵ.

FIG. 5. (Color online) (a) The time dependence of the laser fields $\Omega_{l,1}$ and $\Omega_{l,2}$ when $v/\lambda = 2$ and $\epsilon = 0.258$. (b) Time evolution of the populations for the states $|\psi_1\rangle, |\psi_5\rangle$, and $|\theta_m\rangle$ ($m = 0, 1, \ldots, 5$).

under certain conditions, for an adiabatic system, the oscillation number is in direct proportion to ζ. For fair comparison and to make sure the adiabatic condition for the Hamiltonian in Eq. (17) is fulfilled, it is better to make the population for the same state, i.e., the state $|\varphi_1\rangle$ keeps unchanging with different parameters. We choose population of state $|\varphi_1\rangle$ as a typical example for the analysis. From Eq. (18), the population of state $|\varphi\rangle$ is given by

$$P_1^D = \frac{\lambda^2}{2\Omega_{l,1}^2 + \lambda^2} = \frac{\lambda^2}{2\Xi^2\left(\frac{\cot\epsilon}{t_f}\right)^2 + \lambda^2}, \qquad (28)$$

where $\Xi = (\pi\chi\sin\beta)/v$. To keep P_1^D the same when we change ζ, we change t_f accordingly. $(\cot\epsilon)/t_f = C$ has to be satisfied, where C is a constant. And we obtain

$$\frac{\cot\epsilon}{t_f} = C \Rightarrow t_f = \frac{\cot\epsilon}{C} = \frac{\sqrt{1 - \left(\frac{1}{4\zeta}\right)^2}}{4C\zeta} \simeq \frac{1}{4C\zeta}. \quad (29)$$

The result shows that there is an inverse relationship between the total interaction time t_f and ζ. Therefore, when we choose $\zeta = 2$, for fair comparison, it is better to choose $t_f = 100/\lambda$. In Fig. 6(b), we plot P_j^R and P_j^D again with parameters $\{\zeta = 2, t_f = 100/\lambda, v = 2\lambda\}$. Contrasting Fig. 6(a) with 6(b), we find that when $\zeta = 2$, the oscillation number is double that when $\zeta = 1$, and the more the oscillation number is, the smoother the curve is. When we choose $\zeta = 5$ and $t_f = 250/\lambda$, the curves P_j^R coincide exactly with curves P_j^D as shown in

Fig. 6(c), that is to say, the dark state can describe the evolution governed by $H_{i,s}$ ideally with a relative large ζ. However, a large ζ leads to a small laser amplitude Ω_0, and a small laser amplitude will lead to a long interaction time which is a deviation from our intention.

We contrast the present scheme with adiabatic and Zeno schemes respectively to prove that the STAP has effectively shortened the interaction time. A π phase gate is achieved via adiabatic evolution of dark eigenstates or quantum Zeno dynamics in this two-atom system. The Hamiltonian takes the form in Eq. (5); we only have to change the parameters for the laser pulses. By solving the characteristic equation of H_i the dark state is given by

$$|\text{Dark}(t)\rangle = \frac{1}{N_D}\left[\Omega_{l,2}|\psi_1\rangle - \Omega_{l,1}|\psi_7\rangle \right.$$
$$\left. - \frac{\Omega_{l,1}\Omega_{l,2}}{\lambda}(|\psi_3\rangle - |\psi_5\rangle)\right]. \qquad (30)$$

For simplicity, we also choose the form of the laser pulses as $\Omega_{l,1} = \Omega_0' \sin\beta$ and $\Omega_{l,2} = \Omega_0' \cos\beta$ to meet the boundary conditions for stimulated Raman scattering involving adiabatic passage. When $t = t_f$, $\Omega_{l,1} = -\Omega_0'$, and $\Omega_{l,2} = 0$, and the final state becomes $|\text{Dark}(t_f)\rangle = -|\psi_1\rangle$. Since the adiabatic condition $|\langle\text{Dark}|\partial_t\Phi_{m\neq 0}\rangle| \ll |E_m|$ is too complex to directly analyze, where $|\Phi_m\rangle$ is the mth instantaneous eigenstate corresponding nonzero eigenvalue E_m, we simplify the whole system by setting a limit condition $\Omega_{l,1}, \Omega_{l,2} \ll \lambda, v$ similar to
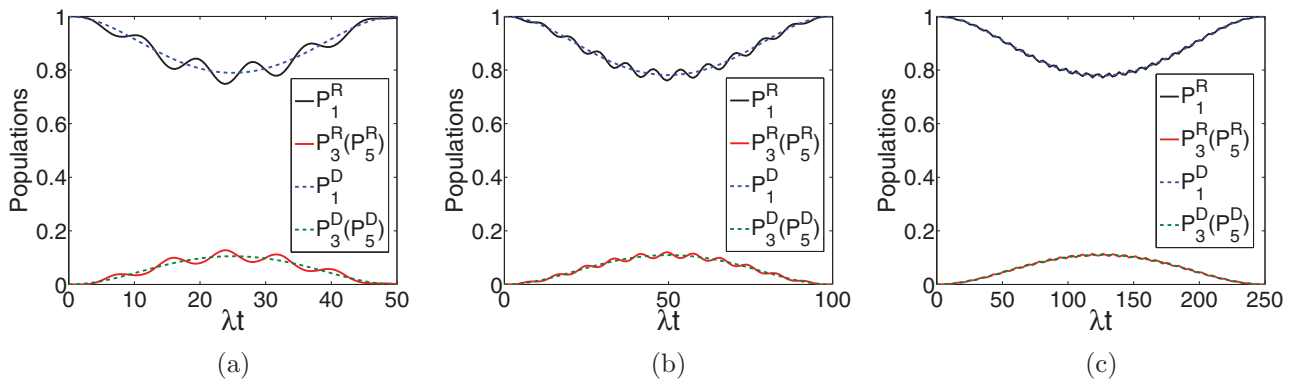

FIG. 6. (Color online) Time evolution of the populations for the states $|\varphi_1\rangle$, $|\varphi_3\rangle$, and $|\varphi_5\rangle$ in different cases: (a) $\zeta = 1$ and $\lambda t_f = 50$; (b) $\zeta = 2$ and $\lambda t_f = 100$; (c) $\zeta = 5$ and $\lambda t_f = 250$.
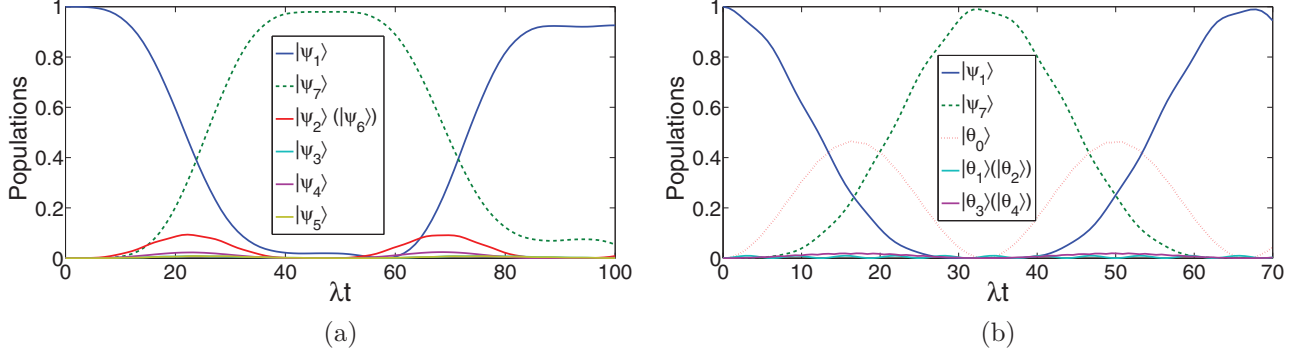
FIG. 7. (Color online) Time-dependent evolution of similar schemes for the π phase gates: (a) via adiabatic passage; (b) via quantum Zeno dynamics.

what we do in Sec. III. Then the Hamiltonian can be simplified as the form in Eq. (9), and the adiabatic condition is also simplified as $|\langle\eta_0|\partial_t\eta_\pm\rangle| \ll |\varepsilon_\pm|$. For the given laser pulses, we have

$$\frac{\dot{\beta}}{\sqrt{2}} \ll \frac{v\Omega_0'}{\chi} \Rightarrow t_f \gg \frac{\pi\chi}{\sqrt{2}v\Omega_0'}. \quad (31)$$

When we choose $v = 2\lambda$, $(\pi\chi)/(\sqrt{2}v\Omega_0') \approx (\Omega_0')^{-1}$. Therefore, the interaction time t_f must be chosen at least 20 times larger than $(\Omega_0')^{-1}$ to obtain a high fidelity of the target state. To prove this, we plot Fig. 7(a) which shows the time evolution of the populations for states $|\psi_1\rangle - |\psi_7\rangle$ when $\Omega_0 = 0.2\lambda$ and $t_f = 100/\lambda = 20(\Omega_0')^{-1}$. Shown in the figure, even with $t_f = 20(\Omega_0')^{-1}$, the adiabatic condition is not ideally fulfilled, the fidelity of the target state $-|\psi_1\rangle$ is only about 92% and states $|\psi_2\rangle$ and $|\psi_6\rangle$ which should have been adiabatically eliminated are populated. That means, if we want to achieve an ideal target state $-|\psi_1\rangle$, the interaction time required in the adiabatic scheme is longer than $20(\Omega_0')^{-1}$. And in a scheme also with Hamiltonian H_i to implement a π phase gate via quantum Zeno dynamics, when the Zeno condition is fulfilled, the evolution of the system is approximatively governed by the effective Hamiltonian in Eq. (9), and the general evolution form of Eq. (9) in time t is

$$|\psi(t)\rangle = \frac{v^2}{(\chi\theta)^2}\left(\Omega_{l,1}^2\cos\theta t + \Omega_{l,2}^2\right)|\psi_1\rangle - i\sin\theta t|\theta_0\rangle,$$
$$+ \frac{v^2}{(\chi\theta)^2}(\Omega_{l,1}\Omega_{l,2}\cos\theta t - \Omega_{l,1}\Omega_{l,2})|\psi_7\rangle, \quad (32)$$

where $\theta = \sqrt{v^2(\Omega_{l,1}^2 + \Omega_{l,2}^2)/\chi^2}$. When we choose $t_f = 2\pi/\theta$ and $\Omega_1 = \Omega_2 = i\Omega_0'$ (Ω_0' is a real number), the final state becomes $|\psi(t_f)\rangle = -|\psi_1\rangle$. As known to all, the smaller the value of Ω_0' is, the better the Zeno condition is satisfied, whereas a smaller Ω_0' leads to a longer operation time. Therefore, we choose a relative large $\Omega_0' = 0.1\lambda$ for the Zeno scheme. In this case, the operation time is $t_f = 2\pi/\theta \approx 21.2\pi/\lambda$ which is a little longer than that of the shortcut scheme when $v = 2\lambda$ as shown in Fig. 7(b). With these parameters, the fidelity of the target state is about 98.9%. It is notable that the state $|\theta_0\rangle$ including atomic excited states is greatly populated which makes the scheme much more sensitive to decoherence caused by atomic spontaneous emission than the shortcut scheme. In general, to avoid this defect, researchers usually create a

detuning between the effective transition $|\psi_1\rangle(|\psi_7\rangle) \leftrightarrow |\theta_0\rangle$ in theory. However, this operation inevitably increases the operation time of the scheme. Limited by the Zeno condition, the present shortcut scheme might not have a distinct advantage in operation time compared with the Zeno scheme, but when all of the merits and faults are considered together, the shortcut scheme is much better than the other two without doubt.

Robustness against possible mechanisms of decoherence is important for a scheme to be applicable in quantum-information processing and quantum computing. It is necessary for us to examine robustness of our shortcut scheme described in the previous sections against decoherence mechanisms including the atomic spontaneous emission, the cavity decay, and the fiber decay. Once the decoherence is considered, the evolution of the system can be modeled by a master equation in Lindblad form,

$$\dot{\rho} = i[\rho, H_i] + \sum_k \left(L_k\rho L_k^\dagger - \frac{1}{2}(L_k^\dagger L_k\rho + \rho L_k^\dagger L_k)\right), \quad (33)$$

where ρ is the density operator for the whole system, and L_k are the so-called Lindblad operators. First, we consider that the initial state is $|\psi_1\rangle$. For the implementation of the π phase gate, there are seven Lindblad operators governing dissipation in the model when the initial state is $|\psi_1\rangle$:

$$L_1^\Gamma = \sqrt{\Gamma_1}|f\rangle_1\langle e|, \quad L_2^\Gamma = \sqrt{\Gamma_2}|f\rangle_2\langle e|,$$
$$L_3^\Gamma = \sqrt{\Gamma_3}|g\rangle_1\langle e|, \quad L_4^\Gamma = \sqrt{\Gamma_4}|g\rangle_2\langle e|, \quad (34)$$
$$L_5^{\kappa_c} = \sqrt{\kappa_1}a_1, \quad L_6^{\kappa_c} = \sqrt{\kappa_2}a_2, \quad L_7^{\kappa_f} = \sqrt{\kappa_f}b,$$

where Γ_i ($i = 1, 2, 3, 4$) are the atomic spontaneous emissions, κ_j ($j = 1, 2$) are the cavity decays, and κ_f is the fiber decay. For simplicity, we set $\Gamma_j = \Gamma/2$ and $\kappa_i = \kappa$. In Fig. 8(a), we plot the fidelity F_1 of the target state $-|\psi_1\rangle$ through the relation $F_1 = |\langle-\psi_1|\rho(t_f)|-\psi_1\rangle|$ versus the dimensionless parameters $\Gamma/\lambda, \kappa/\lambda$ and κ_f/λ via numerically solving the master equation in Eq. (33). We can find from the figure that the method is robust against the cavity decay and fiber decay while sensitive to the atomic spontaneous emission. This result can be understood with the help of Fig. 5(b): the state $|\theta_0\rangle$ including atomic excited states $|\psi_2\rangle$ and $|\psi_4\rangle$ is populated, while the states $|\theta_m\rangle$ ($m = 1, 2, 3, 4$) including cavity- and fiber-excited states remain ignorable during the evolution. Then, if the initial state is $|\varphi_1\rangle$, there will be five Lindblad operators governing
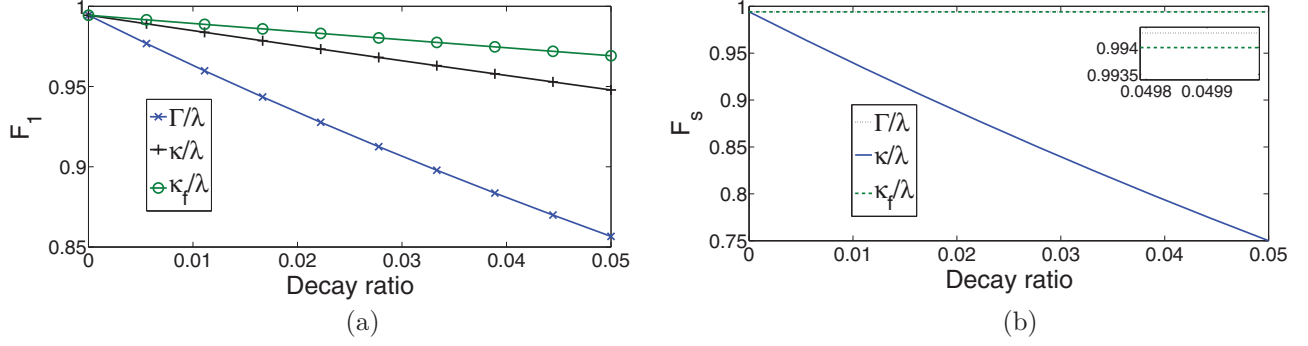
FIG. 8. (Color online) (a) The fidelity F_1 of the target state $-|\psi_1\rangle$ vs the three noise resources Γ/λ, κ/λ, and κ_f/λ. (b) The fidelity F_s of the target state $|\psi_s\rangle$ vs the three noise resources Γ/λ, κ/λ, and κ_f/λ.

dissipation:

$$L_1^\Gamma = \sqrt{\Gamma_1}|f\rangle_1\langle e|, \quad L_2^\Gamma = \sqrt{\Gamma_2}|f\rangle_2\langle e|,$$
$$L_3^{\kappa_c} = \sqrt{\kappa_1}a_1, \quad L_4^{\kappa_c} = \sqrt{\kappa_2}a_2, \quad L_5^{\kappa_f} = \sqrt{\kappa_f}b. \tag{35}$$

We display the dependence on the ratios $\Gamma/\lambda, \kappa/\lambda$, and κ_f/λ of the fidelity of the final state $|\varphi_1\rangle$ through solving the corresponding master equation in Fig. 8(b). The result is much different from that of F_1, when the initial state is $|\varphi_1\rangle$: the atomic spontaneous emissions and the fiber decay almost have no influence on the fidelity while the decay of cavity has great influence. It is because when the initial state is $|\varphi_1\rangle$, the adiabatic condition is fulfilled and the states $|\varphi_2\rangle$ including the atomic-excited state and $|\varphi_4\rangle$ including the fiber-excited state have been effectively adiabatically eliminated. Whereas shorting the operation time requires a relatively large pulse amplitude, so the intermediate states $|\varphi_3\rangle$ and $|\varphi_5\rangle$ in the dark state $|\tilde{\theta}_0\rangle$ including the excited states of the cavity cannot be effectively eliminated during the evolution, and that makes the system sensitive to the cavity decay.

The robustness against operational imperfection is also a main factor for the feasibility of the scheme because most of the parameters are hard to faultlessly achieve in experiment. Hence, we calculate the fidelity by varying error parameters of the mismatch among the laser amplitude, the interaction time, and coupling constants. And we define $\delta x = x' - x$ as the deviation of parameter x. The fidelity versus the variations in different parameters are shown in Fig. 9. As shown in the

figures, the scheme is robust against the variations of λ, v, and T ($T = t_f$ is the total operation time). But it is a little sensitive to the variation of laser amplitude Ω_0 (a deviation $\delta\Omega_0/\Omega_0 = \pm 5\%$ causes a reduction about 3% in the fidelity). That is because the laser amplitude is strongly related to ϵ whose deviation greatly influence the target state's fidelity as shown in Fig. 4. Fortunately, that is not a serious problem to realize the scheme because it is not a challenge to accurately control the laser amplitude in experiment.

In a real experiment, the cesium atoms are applicable to implement the schemes. And an almost perfect fiber-cavity coupling with an efficiency larger than 99.9% can be realized using fiber-taper coupling to high-Q silica microspheres [63]. In the case of that the fiber loss at 852-nm wavelength is only about 2.2 dB/Km [64]; the fiber decay rate is only 0.152 MHz, while in recent experimental conditions [65,66], it is predicted that a strong atom-cavity coupling $\lambda = 2\pi \times 750$ MHz is achieved. That means the fiber decay can actually be neglected in a real experiment with these parameters. And choosing another set of parameters $(\lambda, \Gamma, \kappa) = (2500, 10, 10)$ MHz in the microsphere cavity QED, which is reported in [66,67], the fidelity of the π phase gate is higher than 99%.

VI. CONCLUSION

"Shortcuts to adiabatic passage" has shown its charm in a wide range of applications in quantum information processing and quantum computation. It successfully breaks the time
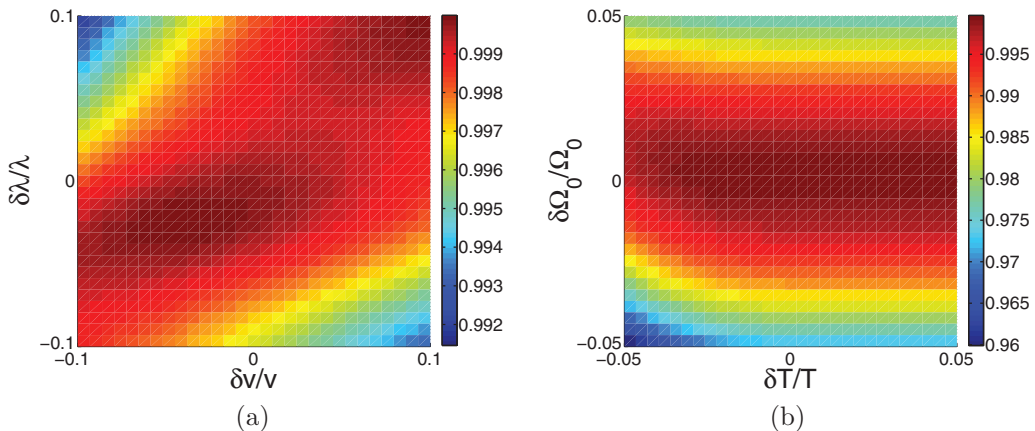

FIG. 9. (Color online) The fidelity F_1 of the target state $-|\psi_1\rangle$ vs the variations of (a) λ and v, (b) Ω_0 and T.

limit in an adiabatic process by providing alternative fast and robust processes which reproduce the same final populations, or even the same final state as the adiabatic process in a finite and shorter time. As we mentioned above, constructing STAPs usually has to deal with the quantum phase transition during the evolution, while how to make use of the phase transition for quantum information processing and computation in cavity QED systems still has not been involved. In this paper, we studied theoretically applications of STAPs for the implementation of π phase gates and the creation of cluster states in distant-atom systems which have advantages in long-distant quantum information processing and quantum computation. Though the interaction time required for the gate operation in the scheme is limited by the Zeno condition, it is still shorter than that in similar schemes via adiabatic passage and quantum Zeno dynamics. Compared with the previous schemes, the present shortcut scheme might be a more reliable choice in experiment, because the scheme is not only fast, but also robust against fluctuations of the parameters and decoherence caused by atomic spontaneous emission and photon loss. In response to the interesting phenomenon that in the adiabatic dark state evolution, the oscillation number is closely related to a special parameter ζ. We have offered analysis and discussion, in as much detail as possible. The paper is promising and might enlighten applications of shortcuts to adiabaticity for quantum phase gates in cavity QED and even other experimental systems.

[1] D. Deutsch, Proc. Roy. Soc. London Ser. A **400**, 97 (1985).

[2] L. K. Grover, Phys. Rev. Lett. **79**, 325 (1997).

[3] P. W. Shor, in *Proceedings of the 35th Annual Symposium on Foundations of Computer Science* (IEEE, New York, 1994).

[4] J. Lee, M. Paternostro, M. S. Kim, and S. Bose, Phys. Rev. Lett. **96**, 080501 (2006).

[5] K. Bergmann, H. Theuer, and B. W. Shore, Rev. Mod. Phys. **70**, 1003 (1998).

[6] P. Král, I. Thanopulos, and M. Shapiro, Rev. Mod. Phys. **79**, 53 (2007).

[7] N. V. Vitanov, T. Halfmann, B. W. Shore, and K. Bergmann, Annu. Rev. Phys. Chem. **52**, 763 (2001).

[8] Z. J. Deng, X. L. Zhang, H. Wei, K. L. Gao, and M. Feng, Phys. Rev. A **76**, 044305 (2007).

[9] L. M. Duan, B. Wang, and H. J. Kimble, Phys. Rev. A **72**, 032333 (2005).

[10] T. Sleator and H. Weinfurter, Phys. Rev. Lett. **74**, 4087 (1995).

[11] D. P. DiVincenzo, Phys. Rev. A **51**, 1015 (1995).

[12] Q. A. Turchette, C. J. Hood, W. Lange, H. Mabuchi, and H. J. Kimble, Phys. Rev. Lett. **75**, 4710 (1995).

[13] C. Monroe, D. M. Meekhof, B. E. King, W. M. Itano, and D. J. Wineland, Phys. Rev. Lett. **75**, 4714 (1995).

[14] J. A. Jones, M. Mosca, and R. H. Hansen, Nature (London) **393**, 344 (1998).

[15] X. Li, Y. Wu, D. Steel, D. Gammon, T. H. Stievater, D. S. Katzer, D. Park, C. Piermarocchi, and L. J. Sham, Science **301**, 809 (2004).

[16] T. Yamamoto, Y. A. Pashkin, O. Astafiev, Y. Nakamura, and J. S. Tsai, Nature (London) **425**, 941 (2004).

[17] C. H. van der Wal, A. C. J. ter Haar, F. K. Wilhelm, R. N. Schouten, C. J. P. M. Harmans, T. P. Orlando, S. Lloyd, and J. E. Mooij, Science **290**, 773 (2000).

[18] J. M. Raimond, M. Brune, and S. Haroche, Rev. Mod. Phys. **73**, 565 (2001).

[19] M. A. Sillanpää, J. I. Park, and R. W. Simmonds, Nature (London) **449**, 438 (2007).

[20] J. Majer, J. M. Chow, J. M. Gambetta, J. Koch, B. R. Johnson, J. A. Schreier, L. Frunzio, D. I. Schuster, A. A. Houck, A. Wallraff, A. Blais, M. H. Devoret, S. M. Girvin, and R. J. Schoelkopf, Nature (London) **449**, 443 (2007).

[21] H. J. Kimble, Nature (London) **453**, 1023 (2008).

[22] J. McKeever, J. R. Buck, A. D. Boozer, A. Kuzmich, H. C. Nägerl, D. M. Stamper-Kurn, and H. J. Kimble, Phys. Rev. Lett. **90**, 133602 (2003).

[23] J. Ye, D. W. Vernooy, and H. J. Kimble, Phys. Rev. Lett. **83**, 4987 (1999).

[24] K. M. Birnbaum *et al.*, Nature (London) **436**, 87 (2005).

[25] A. Rauschenbeutel, G. Nogues, S. Osnaghi, P. Bertet, M. Brune, J. M. Raimond, and S. Haroche, Phys. Rev. Lett. **83**, 5166 (1999).

[26] S. B. Zheng and G. C. Guo, Phys. Rev. Lett. **85**, 2392 (2000).

[27] E. Solano, M. Franca Santos, and P. Milman, Phys. Rev. A **64**, 024304 (2001).

[28] A. Biswas and G. S. Agarwal, Phys. Rev. A **69**, 062306 (2004).

[29] D. Jaksch, J. I. Cirac, P. Zoller, S. L. Rolston, R. Côté, and M. D. Lukin, Phys. Rev. Lett. **85**, 2208 (2000).

[30] S. B. Zheng, Phys. Rev. Lett. **95**, 080502 (2005).

[31] C. P. Yang, S.-I Chu, and S. Han, Phys. Rev. A **70**, 044303 (2004).

[32] X. B. Zou, Y. F. Xiao, S. B. Li, Y. Yang, and G. C. Guo, Phys. Rev. A **75**, 064301 (2007).

[33] S. B. Zheng, Phys. Rev. A **70**, 052320 (2004).

[34] S. B. Zheng, Phys. Rev. A **71**, 062335 (2005).

[35] J. Song, Y. Xia, H. S. Song, J. L. Guo, and J. Nie, Europhys. Lett. **80**, 60001 (2007).

[36] D. Møller, L. B. Madsen, and K. Mølmer, Phys. Rev. A **75**, 062302 (2007).

[37] X. Chen, I. Lizuain, A. Ruschhaupt, D. Guéry-Odelin, and J. G. Muga, Phys. Rev. Lett. **105**, 123003 (2010).

[38] E. Torrontegui, S. Ibáñez, S. Martínez-Garaot, M. Modugno, A. del Campo, D. Gué-Odelin, A. Ruschhaupt, X. Chen, and J. G. Muga, Adv. At. Mol. Opt. Phys. **62**, 117 (2013).

[39] A. Ruschhaupt, X. Chen, D. Alonso, and J. G. Muga, New J. Phys. **14**, 093040 (2012).

[40] A. del Campo, Phys. Rev. A **84**, 031606(R) (2011).

[41] X. Chen, E. Torrontegui, and J. G. Muga, Phys. Rev. A **83**, 062116 (2011).

[42] X. Chen and J. G. Muga, Phys. Rev. A **86**, 033405 (2012).

[43] M. Demirplak and S. A. Rice, J. Phys. Chem. A **107**, 9937 (2003); J. Phys. Chem. B **109**, 6838 (2005); J. Chem. Phys. **129**, 15411 (2008).

[44] M. B. Berry, J. Phys. A: Math. Theor. **42**, 365303 (2009).

[45] J. F. Schaff, X. L. Song, P. Vignolo, and G. Labeyrie, Phys. Rev. A **82**, 033430 (2010).

[46] J. F. Schaff, X. L. Song, P. Capuzzi, P. Vignolo, and G. Labeyrie, Europhys. Lett. **93**, 23001 (2011).

[47] A. Walther, F. Ziesel, T. Ruster, S. T. Dawkins, K. Ott, M. Hettrich, K. Singer, F. Schmidt-Kaler, and U. Poschinger, Phys. Rev. Lett. **109**, 080501 (2012).

[48] R. Bowler, J. Gaebler, Y. Lin, T. R. Tan, D. Hanneke, J. D. Jost, J. P. Home, D. Leibfried, and D. J. Wineland, Phys. Rev. Lett. **109**, 080502 (2012).

[49] S. Y. Tseng and X. Chen, Opt. Lett. **37**, 5118 (2012).

[50] M. G. Bason, M. Viteau, N. Malossi, P. Huillery, E. Arimondo, D. Ciampini, R. Fazio, V. Giovannetti, R. Mannella, and O. Morsch, Nat. Phys. **8**, 147 (2012).

[51] M. Lu, Y. Xia, L. T. Shen, J. Song, and N. B. An, Phys. Rev. A **89**, 012326 (2014).

[52] P. Kwiat, H. Weinfurter, T. Herzog, A. Zeilinger, and M. A. Kasevich, Phys. Rev. Lett. **74**, 4763 (1995).

[53] P. Facchi and S. Pascazio, Phys. Rev. Lett. **89**, 080401 (2002).

[54] Y. H. Chen, Y. Xia, Q. Q. Chen, and J. Song, Phys. Rev. A **89**, 033856 (2014).

[55] Y. H. Chen, Y. Xia, Q. Q. Chen, and J. Song, Laser Phys. Lett. **11**, 115201 (2014).

[56] H. R. Lewis and W. B. Riesenfeld, J. Math. Phys. **10**, 1458 (1969).

[57] M. A. Lohe, J. Phys. A: Math. Theor. **42**, 035307 (2009).

[58] T. Pellizzari, Phys. Rev. Lett. **79**, 5242 (1997).

[59] A. Serafini, S. Mancini, and S. Bose, Phys. Rev. Lett. **96**, 010503 (2006).

[60] Y. Z. Lai, J. Q. Liang, H. J. W. Müller-Kirsten, and J. G. Zhou, Phys. Rev. A **53**, 3691 (1996); J. Phys. A **29**, 1773 (1996).

[61] J. Song, Y. Xia, and H. S. Song, Europhys. Lett. **87**, 50005 (2009).

[62] T. A. Laine and S. Stenholm, Phys. Rev. A **53**, 2501 (1996).

[63] S. M. Spillane, T. J. Kippenberg, O. J. Painter, and K. J. Vahala, Phys. Rev. Lett. **91**, 043902 (2003).

[64] K. J. Gordon, V. Fernandez, P. D. Townsend, and G. S. Buller, IEEE J. Quantum Electron. **40**, 900 (2004).

[65] J. R. Buck and H. J. Kimble, Phys. Rev. A **67**, 033806 (2003).

[66] S. M. Spillane, T. J. Kippenberg, K. J. Vahala, K. W. Goh, E. Wilcut, and H. J. Kimble, Phys. Rev. A **71**, 013817 (2005).

[67] M. J. Hartmann, F. G. S. L. Brandão, and M. B. Plenio, Nat. Phys. **2**, 849 (2006).